Macromolecules

Article

pubs.acs.org/Macromolecules

Tailoring Pore Size and Chemical Interior of near 1 nm Sized Pores in a Nanoporous Polymer Based on a Discotic Liquid Crystal

Subham Bhattacharjee,[†,‡] Jody A. M. Lugger,[†,‡] and Rint P. Sijbesma*[,†,‡]

[†]Laboratory of Molecular Science and Technology and [‡]Institute for Complex Molecular Systems, Eindhoven University of Technology, PO Box 513, 5600 MB, Eindhoven, The Netherlands

Supporting Information

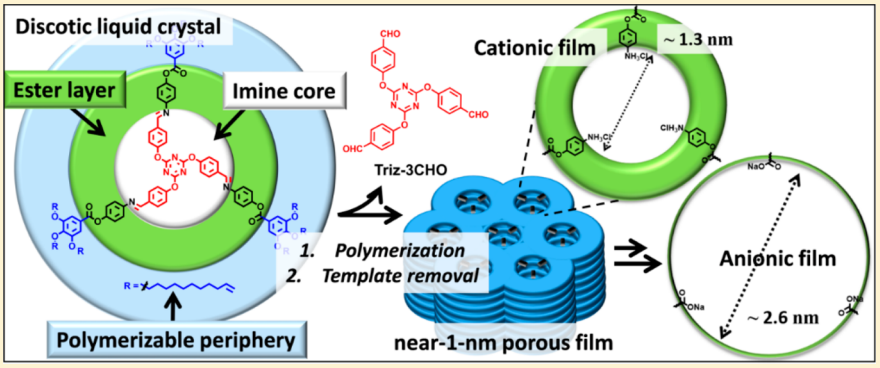

ABSTRACT: A triazine based disc shaped molecule with two hydrolyzable units, imine and ester groups, was polymerized via acyclic diene metathesis in the columnar hexagonal (Col_{hex}) LC phase. Fabrication of a cationic nanoporous polymer (pore diameter ~1.3 nm) lined with ammonium groups at the pore surface was achieved by hydrolysis of the imine linkage. Size selective aldehyde uptake by the cationic porous polymer was demonstrated. The anilinium groups in the pores were converted to azide as well as phenyl groups by further chemical treatment, leading to porous polymers with neutral functional groups in the pores. The pores were enlarged by further hydrolysis of the ester groups to create ~2.6 nm pores lined with −COONa surface groups. The same pores could be obtained in a single step without first hydrolyzing the imine linkage. XRD studies demonstrated that the Col_{hex} order of the monomer was preserved after polymerization as well as in both the nanoporous polymers. The porous anionic polymer lined with −COOH groups was further converted to the −COOLi, −COONa, −COOK, −COOCs, and $-COONH_4$ salts. The porous polymer lined with −COONa groups selectively adsorbs a cationic dye, methylene blue, over an anionic dye.

INTRODUCTION

Nanoporous materials have attractive properties for a wide variety of applications in adsorption and separation.[1,2] The presence of a high density of pores with well-defined dimensions[3−5] gives these materials superior capacity, an increased surface area, and higher selectivity than mesoporous materials.

The fabrication of nanoporous materials has two distinct approaches: top-down fabrication, where the pores are introduced by manipulating a pristine material, and fabrication using self-assembly, where the nanostructure is an intrinsic feature of the material.[5,6] Nanoporous materials based on polymers and organic molecules have been prepared via a range of top-down methods, but the use of self-assembly is attractive because it potentially leads to highly efficient manufacturing processes and can perhaps access even smaller features. A widely used strategy to make self-assembled nanostructured materials is to use microphase separation in block copolymers. When this strategy is combined with selective removal of one of the blocks, nanoporous materials with pores down to 5−10 nm are obtained.[8,9] Nanostructured materials with considerably smaller features than 5 nm have been obtained from liquid crystalline (LC) building blocks.[5,10−12]

In columnar LC phases of disk shaped molecules or complexes, features below 2 nm are usually present.[13,14] Polymerization of these phases followed by selective removal of the core of the disk is a powerful and effective method for the preparation of nanoporous polymer films. Such films, which combine very small pore sizes with a high pore density, are of interest because they are expected to have favorable properties for many application, e.g., water desalination or as ion selective membranes in batteries.[12,13]

The scope of nanoporous materials is significantly broadened by chemical modification of the pore surface, which is common practice for zeolites, porous carbon materials, and covalent organic frameworks.[14−16] The pore interior of top-down

Received: January 5, 2017
Revised: March 6, 2017
Published: March 23, 2017

DOI: 10.1021/acs.macromol.7b00013
Macromolecules 2017, 50, 2777−2783

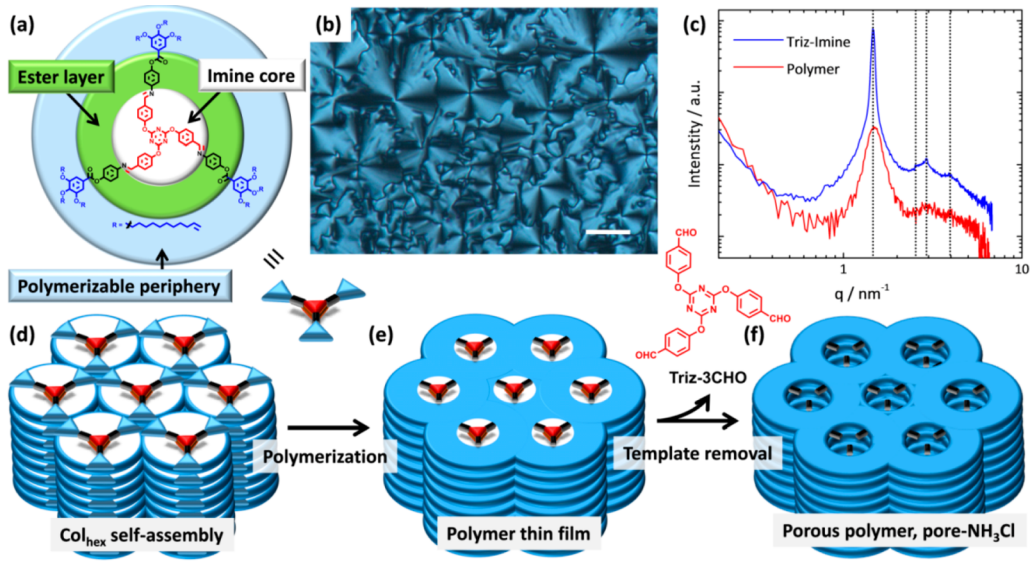

Figure 1. (a) Chemical structure of the triazine based disk shaped molecule, Triz-Imine. (b) POM of Triz-Imine at 75 °C, showing a focal conic texture typical for a Col_{hex} phase. Picture obtained during cooling from the isotropic state at a rate of 0.1 °C/min (scale bar represents 200 μm). (c) Medium angle XRD pattern of the monomer Triz-Imine and its polymer. (d) Schematic illustrations of the formation of the Col_{hex} phase by Triz-Imine, (e) its polymerization in the LC phase using Grubbs' catalyst, second generation, and (f) subsequent template removal by hydrolyzing the imine linkage using DMF:HCl (11:1 v/v) to fabricate the porous polymer, Pore-NH_3Cl, with amine functional groups at the pore surface.

fabricated nanochannels in thin films has been chemically modified to tune their mode of selectivity to discriminate on the basis of size, charge, wettability, recognition, or a combination of these properties.[17,18]

Pore surface functionalization of nanoporous materials based on self-assembled block copolymer has also been explored; e.g., the group of Hillmyer reported the conversion of pores lined with carboxylic acids to amides using coupling reagents and three different amines, whereas in another study pores lined with alkene units were successfully converted to epoxides.[19,20] Other examples report e.g. the preparation of quaternary pyridinium salts in pores lined with polymer segments or the formation of pores lined with carboxylate groups after the hydrolysis of dimethylacrylamide groups.[24,25] It is known that LC based nanoporous materials can selectively adsorb small molecules;[2,13,26] however, covalent pore surface functionalization has not been reported yet for LC based nanoporous networks and would constitute a distinct step forward in the development of functional nanoporous polymers based on LCs because it creates a handle in the pore facilitating modification of the chemical environment of the pore lining. We expect that this additional functionality will provide crucial tunability of LC based nanoporous films for specific applications. In addition to tuning the exact size of the pore, the chemical environment is also modified and affects properties such as flux, selectivity, and rejection, which depend on the interplay between pore size and the chemical environment.[20,27]

Fabrication of nanoporous polymer films based on a noncovalent templated liquid crystal, polymerized via alkene metathesis, has been illustrated previously.[13] Facile pore surface functionalization of such materials would be a distinct step forward to functional nanoporous membranes.

Herein, we report on the design and synthesis of a discotic molecule with a triazine core and nine terminal alkene groups at the periphery. The molecules are designed to polymerize through dimerization of alkene groups using acyclic diene metathesis (ADMET)[28,29] in the Col_{hex} LC phase without affecting structural organization of the disks in the LC phase. The imine and ester groups provide two hydrolyzable units (Figure 1) for stepwise removal of the inner imine and outer ester core from each disc of the polymer to introduce amine-functionalized smaller cationic pores (pore diameter ~1.3 nm) and carboxylate-functionalized bigger anionic pores (pore diameter ~2.6 nm) in the polymer film. The amine and carboxylate functional groups at the pore wall are amenable to chemical conversion to other functionalities. In addition, the porous polymer with charged moieties at the pore surface is well suited to selectively adsorb oppositely charged dyes.

RESULTS AND DISCUSSION

LC Properties of Triz-Imine. The thermotropic LC properties of the Triz-Imine were investigated with differential scanning calorimetry (DSC), X-ray diffraction (XRD), and polarizing optical microscopy (POM). DSC showed a broad endothermic peak at 64.3 °C (ΔH = 2.65 J/g), indicating a crystalline to LC phase transition (Figure 2a). The sample remains in the LC phase until it melts at 88.6 °C (ΔH = 0.26 J/g) and returns to the LC phase when cooled to 86 °C from the isotropic melt. When heated under POM, the sample was birefringent between 64 and 86 °C (Figure S1a). A focal conic texture typical for a Col_{hex} phase could be grown from the isotropic melt on cooling the sample at a rate of 0.1 °C/min, indicating the presence of an enantiotropic LC phase (Figure 1b and Figure S1b,c).[13] The LC phase was further characterized by recording variable temperature XRD (Figure 1c). Diffraction peaks with q-ratios of $1:\sqrt{3}:\sqrt{4}$ were observed both during the heating and cooling cycle at 75 °C, which confirms the existence of a disordered Col_{hex} phase with a disk diameter of 4.95 nm.[13]

Fixation of the LC Morphology via ADMET. Solutions of Triz-Imine (10 mg/30 μL $CHCl_3$) and Grubbs' catalyst, second generation (0.2 mg/20 μL $CHCl_3$), were prepared separately. The solutions were mixed and dried in a high vacuum for 25–30 s and then kept in a vacuum oven at 75 °C for 12 h to

DOI: 10.1021/acs.macromol.7b00013
Macromolecules 2017, 50, 2777–2783

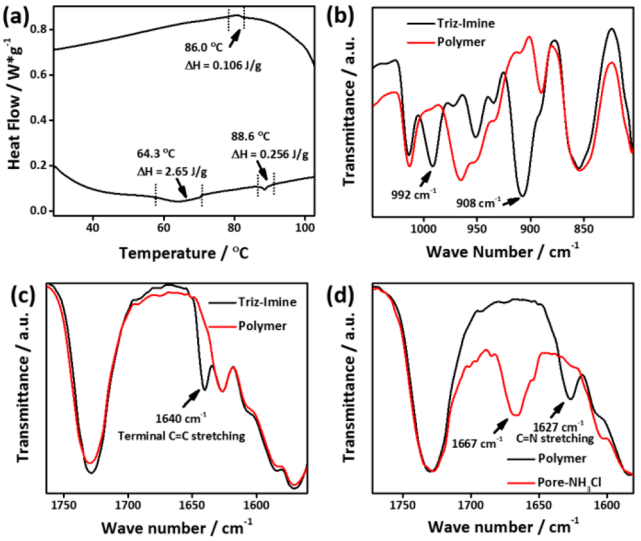

Figure 2. (a) DSC thermogram of Triz-Imine. (b, c) FT-IR spectra of the monomer Triz-Imine and its polymer. (d) Comparison of the FT-IR spectra of the native polymer and the porous polymer, Pore-NH_3Cl.

polymerize the terminal double bonds via ADMET.[29] FT-IR analysis showed high conversion as the end-terminal =C−H bending vibration band at 908 and 992 cm^{-1} of Triz-Imine had disappeared completely after polymerization (Figure 2b).[13] The polymer film with a thickness in the range of 6−25 μm did not show a terminal C=C stretching vibration band at 1640 cm^{-1}, which is clearly visible in the FT-IR spectrum of Triz-imine (Figure 2c). In addition, the intensity of the vinylic =C−H stretching vibration band at 3077 cm^{-1} was strongly reduced in the polymer compared to Triz-Imine (Figure S2). The data show high conversion of terminal to internal alkenes. Insolubility of the polymer film in $CHCl_3$, EtOH, DMF, DMF:HCl (11:1 v/v), and acetic acid confirmed the high degree of cross-linking.

The XRD diffraction patterns of Triz-Imine after ADMET polymerization showed retention of the hexagonal lattice (Figure 1c). The lattice spacing, d_{100}, was slightly decreased from 4.29 to 4.21 nm after polymerization. Although the d_{110} and d_{200} reflections could no longer be observed separately in the polymerized film due to broadening, this indicates that terminal alkene metathesis reaction is enough to form a cross-linked polymer network and fixate the morphology of the LC phase.

Nanoporous Polymer Film Fabrication via Template Removal. After the polymerization of Triz-Imine, the imine linkages in the polymer were hydrolyzed in DMF:HCl, which was a good solvent for the subsequent removal of the template aldehyde Triz-3CHO from the polymer. For template hydrolysis and removal, a polymer sample was shaken gently overnight at room temperature in DMF:HCl (11:1 v/v). UV/vis absorption spectra of the solutions showed that after two extractions the template had been quantitatively removed (Figure S3). This was confirmed by the disappearance of the C=N stretching vibration at 1627 cm^{-1} in the FT-IR spectrum of the polymer (Figure 2d).[30] An N−H stretching band of $-NH_3Cl$ functional groups of the anilinium salt in the pores was not observed in the FT-IR spectrum, presumably because of spectral overlap.

Performing XRD on the films showed that the diffraction pattern of the porous polymer was the same as the native polymer film. However, the lattice spacing, d_{100}, increased from

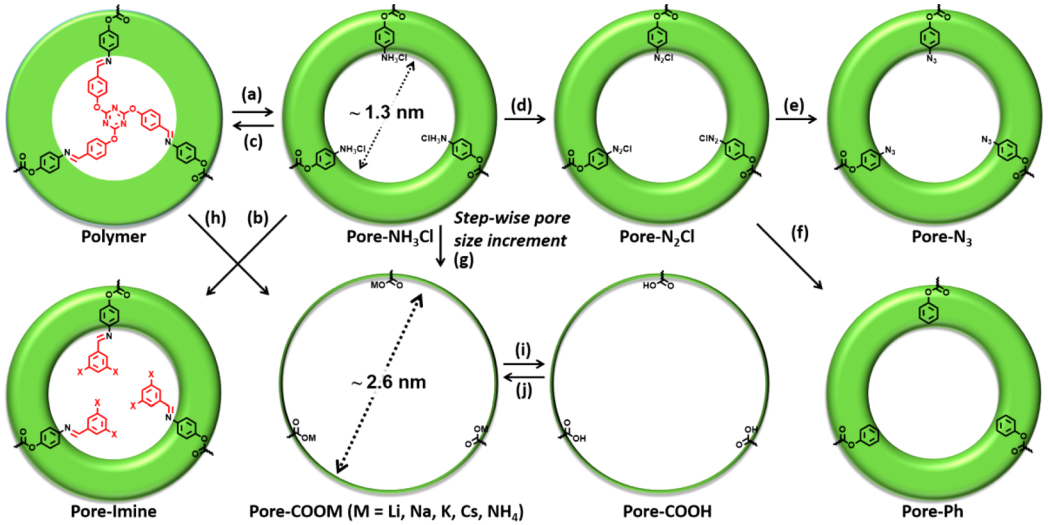

Figure 3. Schematic illustrations of the pore surface engineering of the porous polymers: (a) Hydrolysis of the imine linkage of the native polymer using DMF:HCl (11:1 v/v) to fabricate the porous polymer, Pore-NH_3Cl. The amino groups in the pores reacted with different aldehydes, (b) benzaldehyde (where X = H), benzene-1,3,5-tricarboxaldehyde (where X = CHO), and (c) the template aldehyde, Triz-3CHO, to transform back to the original polymer. (d) The ammonium groups in the pores of Pore-NH_3Cl were converted to diazonium salt ($-N_2Cl$) by reacting with aqueous $NaNO_2$/HCl solution at 0−5 °C for 1 h. (e, f) Pore-N_2Cl was further reacted with NaN_3 and H_3PO_2 in water and THF, respectively, at 21 °C to fabricate porous polymers with neutral azide ($-N_3$) and phenyl (−Ph) groups at the pore surface (Pore-N_3 and Pore-Ph), respectively. (g) The ester groups present in the inner core of Pore-NH_3Cl were successfully hydrolyzed using 1 M NaOH in EtOH:H_2O (23:1 v/v) at 75 °C for 12 h to furnish a porous polymer containing anionic −COONa groups at the pore surface. (h) Pore-COONa could be directly obtained in one step by reacting the native polymer with 1 M NaOH in EtOH:H_2O (23:1 v/v) at 75 °C for 12 h. (i) Pore-COONa was converted to a porous polymer with −COOH groups at the pore surface (Pore-COOH) by reacting with ethanolic HCl solution for 10−12 min at ambient condition. (j) Treatment of Pore-COOH with hydroxides salt of Li^+, Na^+, K^+, Cs^+, and NH_4^+ resulted in the formation of Pore-COOM (where M = Li, Na, K, Cs, and NH_4).

DOI: 10.1021/acs.macromol.7b00013
Macromolecules 2017, 50, 2777−2783

4.21 to 4.39 nm upon removal of the template, which we attributed to the reduction of the cross-link density and concomitant stress relaxation (Figure 4c). This result indicates structural integrity and the formation of nanopores with an estimated pore diameter of ~1.3 nm (Figure 3, path a, and Figure S4).

After drying the porous polymer under vacuum (<1 mbar) at 21 °C for 2 days, a relatively broad absorption band at 1667 cm^{-1} persisted in the FT-IR spectrum, which was assigned to the C═O stretching vibration of DMF (Figure 2c). In line with the porosity of the polymerized material, DMF molecules were strongly H-bonded with the $-NH_3Cl$ surface groups in the pores and retained in the porous polymer, Pore-NH_3Cl.

Thermogravimetric analysis (TGA) of the porous polymer showed around 4% weight loss at 145 °C, a temperature at which the polymer and the catalyst embedded in the polymer are stable (Figure S5a). The native polymer before template removal showed no weight loss at that temperature (Figure S5b). The 4% weight loss of DMF indicates the presence of approximately 1 molecule of DMF per disk in Pore-NH_3Cl. The adsorbed DMF molecules could be removed, however, by soaking the polymer in MeOH for 24 h at room temperature, followed by drying (Figure S6a).

Selective Uptake of Aldehydes. The $-NH_3Cl$ groups at the pore surface were converted to imines by reacting with different aldehydes in THF at room temperature, with a trace of acetic acid as catalyst. Reaction of Pore-NH_3Cl with benzaldehyde (Ben-CHO), resulted in an imine, as was evident from the reappearance of the C═N stretching absorption at 1627 cm^{-1} (Figure 4a), while the band of pore-adsorbed DMF at 1667 cm^{-1} was reduced in intensity after the reaction. It is noteworthy to mention that the native polymer before template removal did not swell in DMF. The FT-IR spectrum of the native polymer soaked with DMF for 24 h only has a minor band at 1678 cm^{-1} which can be ascribed to surface bound DMF (Figure S6b). In addition, we did not see swelling of the sample by eye.

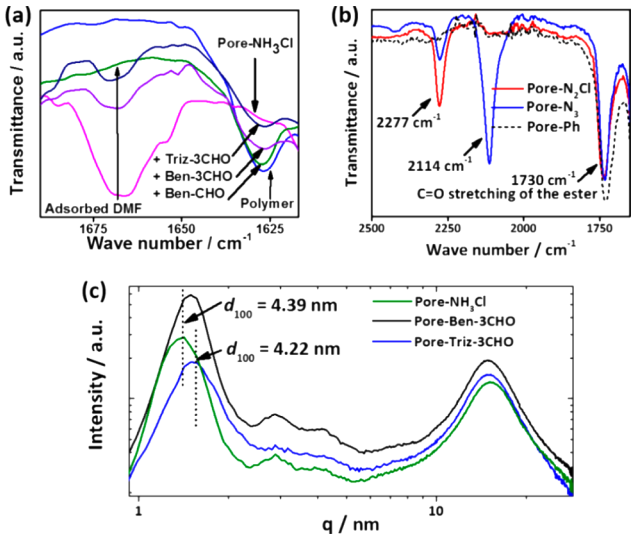

Figure 4. (a) FT-IR spectra of the nonporous polymer, the porous polymer film, Pore-NH_3Cl, and after reacting Pore-NH_3Cl with different aldehydes. (b) FT-IR spectra of the diazonium lined porous polymer, Pore-N_2Cl, and its further modification to the porous polymers containing azide ($-N_3$) and phenyl (−Ph) groups at the pore surface (Pore-N_3 and Pore-Ph). (c) Wide-angle XRD patterns of the porous polymer film, Pore-NH_3Cl, and after reacting Pore-NH_3Cl with benzaldehyde and Triz-3CHO.

The $-NH_3Cl$ groups were not fully converted when benzene-1,3,5-tricarbaldehyde (Ben-3CHO) was used as the reactant, even though it has three reactive aldehyde groups and is smaller than the initial template (Figure 4a). In addition, the presence of a band at ~1700 cm^{-1} in FT-IR, which is not present when reacted with benzaldehyde, suggests that unreacted aldehyde groups are present in the resulting polymer film (Figure S6c). The amino groups lining the pores also react only partially with the larger Triz-3CHO, the trialdehyde that was used as template (Figure 4a). Under identical conditions, the polymer film did not react at all with the smaller 1-pyrenecarboxaldehyde (Figure S6d), indicating that imine formation is dependent on more than just the size of the aldehyde. In addition, the anionic dye sodium fluorescein (SF) was also not taken up in the cationic pores probably because of its larger size (Figure S6e).

The porous polymers functionalized with different aldehydes were further characterized with XRD (Figure 4c). The d_{100} lattice spacing decreased slightly from 4.39 to 4.22 and 4.13 nm for the films treated with benzaldehyde and Triz-3CHO, respectively, while the diffraction patterns remained the same.

Pore Surface Engineering: Diazonium Functionalized Pore Surface. The presence of primary amines opens up multiple possibilities to modify the pore surface by further chemical transformations, for which the diazonium group is a convenient intermediate. Amine groups in the pores were converted to the diazonium salt with $NaNO_2$ in cold aqueous HCl solution. The resulting film showed a strong absorption band at 2277 cm^{-1} (Figure 4b), characteristic of the $-N_2^+$ group, confirming the formation of diazonium groups in the pores, Pore-N_2Cl, (Figure 3, path d).[31] The ester groups in the polymer did not hydrolyze during the diazotization reaction as is indicated by the persistence of the ester C═O stretching band at 1730 cm^{-1}. The $-N_2Cl$ group, a relatively unstable intermediate when in solution, showed remarkable stability in the film, where it decomposes only partially after 20 days at room temperature as evidenced from the FT-IR analysis (Figure S7a).

Hydrophobic Pores Lined with Azide and with Phenyl Groups. Treatment of the porous polymer, Pore-N_2Cl, with aqueous NaN_3 resulted in conversion of the $-N_2^+$ groups to $-N_3$ groups. The intensity of the absorption band at 2277 cm^{-1} ascribed to the $-N_2^+$ stretching vibration decreased considerably at the expense of a new band at 2114 cm^{-1} (Figure 4b), which confirms the formation of porous polymer, Pore-N_3, with azide functionalized neutral pores (Figure 3, path e).[32] The $-N_2^+$ groups in the pores were also replaced with protons by reaction with H_3PO_2 in THF at room temperature (Figure 3, path f, and Figure 4b).

Stepwise Pore Size Increment of the Small Cationic Pores to Larger Anionic Pores. The porous polymer, Pore-NH_3Cl, contains ester groups in the core (Figure 1a). The small cationic pores were converted to bigger anionic pores by hydrolysis of the ester groups. To this end, the porous polymer was treated with 1 M NaOH in EtOH:H_2O (23:1 v/v) at 75 °C overnight. Analysis of the FT-IR spectrum of the resultant polymer showed the C═O stretching vibration at 1730 cm^{-1} and the peak for DMF (1667 cm^{-1}) had disappeared in the resultant film, with the emergence of two new absorption peaks at 1556 and 1404 cm^{-1} (Figure 5a), assigned to asymmetric and symmetric C═O stretching vibrations of −COONa groups,

DOI: 10.1021/acs.macromol.7b00013
Macromolecules 2017, 50, 2777−2783

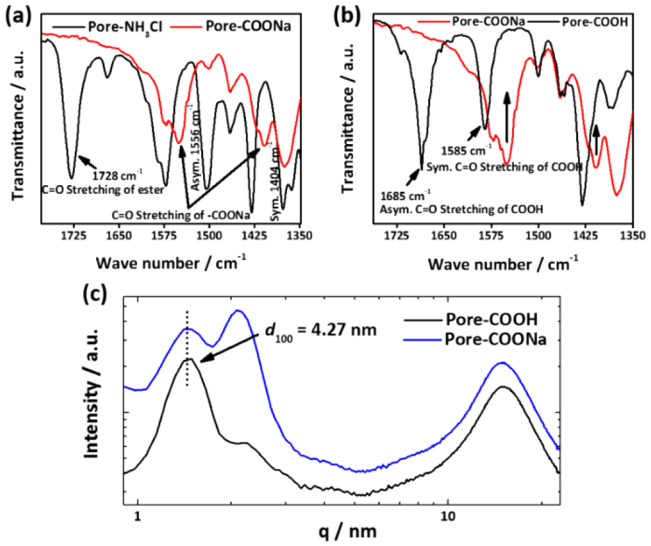

Figure 5. FT-IR spectra depicting (a) the transformation of Pore-NH_3Cl to an anionic porous polymer, Pore-COONa, and (b) the conversion of the porous polymer, Pore-COONa, to Pore-COOH. (c) XRD patterns of the porous polymers, Pore-COONa and Pore-COOH.

respectively.[13] Therefore, we have been able to convert the cationic small pores (diameter ~1.3 nm) to anionic bigger ones (diameter ~2.6 nm) (Figure 3, path g).

Direct treatment of the native polymer with 1 M NaOH in EtOH:H_2O (23:1 v/v) at 75 °C for 12 h led to a one-step removal of the core template as the resultant polymer showed same FT-IR absorption spectrum as that of Pore-COONa (Figure 3, path h, and Figure S7b).

The porous polymer, Pore-COONa, was further treated with EtOH:HCl (11:1 v/v) for 10−12 min at 21 °C. As a result, the asymmetric and symmetric C═O stretching vibration of −COONa groups shifted from 1556 to 1685 and 1404 to 1585 cm^{-1}, respectively, indicating formation of pores with a −COOH groups at the surface (Figure 3, path i, and Figure 5b).[13] The structural integrity in Pore-COONa and Pore-COOH was retained without collapsing the pores as was evident from the XRD patterns (Figure 5c).

Anionic Porous Polymer with Different Counter Cations in the Pore. Films of Pore-COOH were treated with 1 M solutions of the hydroxide salts of Li^+, Na^+, K^+, Cs^+ and NH_4^+ ions in EtOH:H_2O (23:1 v/v) for 2 h. After treatment, the asymmetric and symmetric stretching band of −COOH have shifted from 1685 to 1560 cm^{-1} and from 1585 to 1404 cm^{-1}, respectively (Figure S7c). The data clearly indicates the formation of a porous polymer lined with −COOLi, −COONa, −COOK, −COOCs, and −$COONH_4$ functional groups at the pore surface (Figure 3, path j). In this regard, it is important to mention that we previously reported selective binding of Na^+ and K^+ ions among hydroxide salts in −COOH functionalized porous polymer with a pore diameter of ~1.6 nm, while in the present case, also Cs^+ ions were taken up as a countercation in the bigger anionic pores.[13]

Selective Dye Adsorption Studies. The anionic pores in Pore-COONa are likely to selectively adsorb cationic dyes. To check this hypothesis, adsorption of cationic and anionic dyes was studied. Methylene blue (MB), a cationic dye, was found to be adsorbed from its aqueous solution when Pore-COONa was immersed in 10 μM aqueous solution of MB, 1.5 mL. Dye adsorption was monitored by recording UV/vis spectra of the solution at different time intervals (Figure 6a). MB was

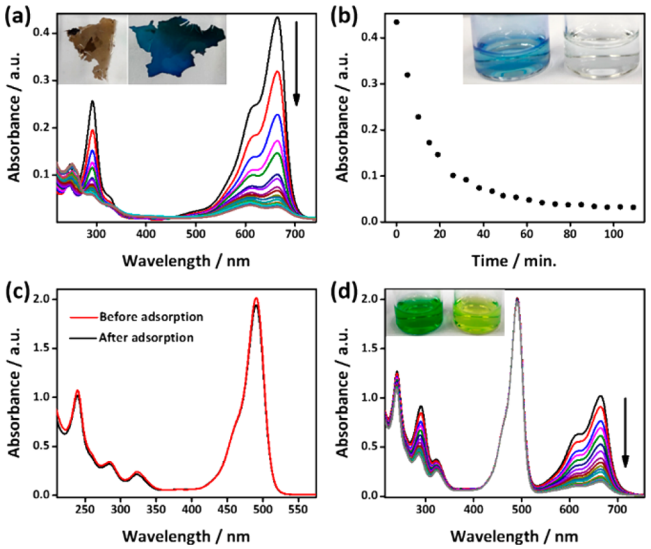

Figure 6. (a) Monitoring adsorption of the cationic dye, MB (10 μM), by the −COONa functionalized anionic pores of Pore-COONa, in aqueous medium using UV/vis absorption spectroscopy and (b) the plot of absorbance at 665 nm versus time. The inset in parts a and b showing the color of the porous polymer, Pore-COONa and MB solution before and after adsorption experiment, respectively. (c) UV/vis absorption spectra of the anionic dye, SF, solution before and after exposure to Pore-COONa. (d) Selective adsorption of the cationic dye, MB, over the anionic dye, SF, by Pore-COONa was monitored by the UV/vis spectroscopy. The inset in part d showing the color of the [MB (20 μM) + SF (30 μM)] solution before and after adsorption by Pore-COONa.

adsorbed rapidly by the porous polymer, turning the solution from deep blue to nearly colorless, while the porous polymer became bluish (Figures 6a and 6b, insets), adsorption reached a plateau within 1 h as determined from the decrease of the absorption intensity at 665 nm (Figure 6b). After saturation with MB from a 10 μM aqueous solution over 12 h, approximately 13% of the −COONa groups was associated with a dye molecule (Figure S8).

In contrast, hardly any of the anionic dye, sodium fluorescein (SF), was adsorbed from an aqueous solution by Pore-COONa (Figure 6c). Ion selectivity is illustrated by treating a mixture of SF and MB with Pore-COONa, the green solution (MB plus SF) turned yellow-green (the color of an SF solution) after the treatment with the anionic material (Figure 6d).

CONCLUSIONS

The fabrication of nanoporous polymers by hydrolysis of the discotic core from a polymerized LC-film has been demonstrated. Pore-NH_3Cl (pore diameter ~1.3 nm), with ammonium groups in the pore interior, reacts faster with smaller aldehydes than with larger ones, but reactivity is not determined by size alone. The ammonium groups in Pore-NH_3Cl were successfully converted to the diazonium salt, which is shown to be a versatile reactive intermediate for further chemical modification of the pores.

A nanoporous material, Pore-COONa, with larger, anionic functionalized pores of ~2.6 nm was obtained either from Pore-NH_3Cl or directly in one step from the native polymer thin

DOI: 10.1021/acs.macromol.7b00013
Macromolecules 2017, 50, 2777−2783

film. Selective adsorption of cationic over anionic dyes in the anionic pores of Pore-COONa was demonstrated. The cations in Pore-COONa could be exchanged by converting to the carboxylic acid, followed by treatment with the hydroxides of Li^+, Na^+, K^+, Cs^+, and NH_4^+. The demonstrated possibility to covalently modify the pore surface in nanometer sized pores of a polymer thin film offers ample opportunities to develop functional materials. We believe that the present strategy, to modify the pore surface, can be extended to other functions. Further pore surface engineering, adsorption, and filtration studies with these porous materials are under way.

■ ASSOCIATED CONTENT

Supporting Information

The Supporting Information is available free of charge on the ACS Publications website at DOI: 10.1021/acs.macromol.7b00013.

Synthesis, detailed experimental procedures, and Figures S1−S8 (PDF)

■ AUTHOR INFORMATION

Corresponding Author

*E-mail: R.P.Sijbesma@tue.nl (R.P.S.).

ORCID

Rint P. Sijbesma: 0000-0002-8975-636X

Author Contributions

S.B. and J.A.M.L. contributed equally.

Funding

This research is supported by the Ministry of Education, Culture and Science of The Netherlands (Gravity program 024.001.035) and partly financed by The Netherlands Organisation for Scientific Research (NWO), project number 729.002.003.

Notes

The authors declare no competing financial interest.

■ ACKNOWLEDGMENTS

We thank Anne Hélène Gelebart for suggesting and performing the TGA analysis.

■ REFERENCES

(1) Surwade, S. P.; Smirnov, S. N.; Vlassiouk, I. V.; Unocic, R. R.; Veith, G. M.; Dai, S.; Mahurin, S. M. Water Desalination Using Nanoporous Single-Layer Graphene. *Nat. Nanotechnol.* **2015**, *10* (5), 459−464.

(2) van Kuringen, H. P. C.; Eikelboom, G. M.; Shishmanova, I. K.; Broer, D. J.; Schenning, A. P. H. J. Responsive Nanoporous Smectic Liquid Crystal Polymer Networks as Efficient and Selective Adsorbents. *Adv. Funct. Mater.* **2014**, *24* (32), 5045−5051.

(3) Schenning, A. P. H. J.; Gonzalez-Lemus, Y. C.; Shishmanova, I. K.; Broer, D. J. Nanoporous Membranes Based on Liquid Crystalline Polymers. *Liq. Cryst.* **2011**, *38* (11−12), 1627−1639.

(4) Zhang, Y.; Sargent, J. L.; Boudouris, B. W.; Phillip, W. A. Nanoporous Membranes Generated from Self-Assembled Block Polymer Precursors: Quo Vadis? *J. Appl. Polym. Sci.* **2015**, *132* (21), 41683.

(5) Henmi, M.; Nakatsuji, K.; Ichikawa, T.; Tomioka, H.; Sakamoto, T.; Yoshio, M.; Kato, T. Self-Organized Liquid-Crystalline Nanostructured Membranes for Water Treatment: Selective Permeation of Ions. *Adv. Mater.* **2012**, *24* (17), 2238−2241.

(6) Yu, H.-D.; Regulacio, M. D.; Ye, E.; Han, M.-Y. Chemical Routes to Top-down Nanofabrication. *Chem. Soc. Rev.* **2013**, *42* (14), 6006−6018.

(7) Ozin, G. A.; Hou, K.; Lotsch, B. V.; Cademartiri, L.; Puzzo, D. P.; Scotognella, F.; Ghadimi, A.; Thomson, J. Nanofabrication by Self-Assembly. *Mater. Today* **2009**, *12* (5), 12−23.

(8) Sinturel, C.; Bates, F. S.; Hillmyer, M. A. High χ−Low N Block Polymers: How Far Can We Go? *ACS Macro Lett.* **2015**, *4* (9), 1044−1050.

(9) Hillmyer, M. A. Nanoporous Materials from Block Copolymer Precursors. In *Block Copolymers II*; Abetz, V., Ed.; Advances in Polymer Science; Springer: Berlin, 2005; pp 137−181.

(10) Kato, T.; Yasuda, T.; Kamikawa, Y.; Yoshio, M. Self-Assembly of Functional Columnar Liquid Crystals. *Chem. Commun.* **2009**, No. 7, 729−739.

(11) Feng, X.; Tousley, M. E.; Cowan, M. G.; Wiesenauer, B. R.; Nejati, S.; Choo, Y.; Noble, R. D.; Elimelech, M.; Gin, D. L.; Osuji, C. O. Scalable Fabrication of Polymer Membranes with Vertically Aligned 1 nm Pores by Magnetic Field Directed Self-Assembly. *ACS Nano* **2014**, *8* (12), 11977−11986.

(12) Kishikawa, K.; Hirai, A.; Kohmoto, S. Fixation of Multilayered Structures of Liquid-Crystalline 2:1 Complexes of Benzoic Acid Derivatives and Dipyridyl Compounds and the Effect of Nanopillars on Removal of the Dipyridyl Molecules from the Polymers. *Chem. Mater.* **2008**, *20* (5), 1931−1935.

(13) Bögels, G. M.; Lugger, J. A. M.; Goor, O. J. G. M.; Sijbesma, R. P. Size-Selective Binding of Sodium and Potassium Ions in Nanoporous Thin Films of Polymerized Liquid Crystals. *Adv. Funct. Mater.* **2016**, *26*, 8023−8030.

(14) Lee, H.-K.; Lee, H.; Ko, Y. H.; Chang, Y. J.; Oh, N.-K.; Zin, W.-C.; Kim, K. Synthesis of a Nanoporous Polymer with Hexagonal Channels from Supramolecular Discotic Liquid Crystals. *Angew. Chem., Int. Ed.* **2001**, *40* (14), 2669−2671.

(15) Cohen-Tanugi, D.; Grossman, J. C. Water Desalination across Nanoporous Graphene. *Nano Lett.* **2012**, *12* (7), 3602−3608.

(16) Ye, J.; Baumgaertel, A. C.; Wang, Y. M.; Biener, J.; Biener, M. M. Structural Optimization of 3D Porous Electrodes for High-Rate Performance Lithium Ion Batteries. *ACS Nano* **2015**, *9* (2), 2194−2202.

(17) Chudasama, C. D.; Sebastian, J.; Jasra, R. V. Pore-Size Engineering of Zeolite A for the Size/Shape Selective Molecular Separation. *Ind. Eng. Chem. Res.* **2005**, *44* (6), 1780−1786.

(18) Stein, A.; Wang, Z.; Fierke, M. A. Functionalization of Porous Carbon Materials with Designed Pore Architecture. *Adv. Mater.* **2009**, *21* (3), 265−293.

(19) Nagai, A.; Guo, Z.; Feng, X.; Jin, S.; Chen, X.; Ding, X.; Jiang, D. Pore Surface Engineering in Covalent Organic Frameworks. *Nat. Commun.* **2011**, *2*, 536.

(20) Zhang, H.; Tian, Y.; Jiang, L. Fundamental Studies and Practical Applications of Bio-Inspired Smart Solid-State Nanopores and Nanochannels. *Nano Today* **2016**, *11* (1), 61−81.

(21) Small, L. J.; Wheeler, D. R.; Spoerke, E. D. Nanoporous Membranes with Electrochemically Switchable, Chemically Stabilized Ionic Selectivity. *Nanoscale* **2015**, *7* (40), 16909−16920.

(22) Rzayev, J.; Hillmyer, M. A. Nanochannel Array Plastics with Tailored Surface Chemistry. *J. Am. Chem. Soc.* **2005**, *127* (38), 13373−13379.

(23) Bailey, T. S.; Rzayev, J.; Hillmyer, M. A. Routes to Alkene and Epoxide Functionalized Nanoporous Materials from Poly(styrene-B-Isoprene-B-Lactide) Triblock Copolymers. *Macromolecules* **2006**, *39* (25), 8772−8781.

(24) Rao, J.; Ma, H.; Baettig, J.; Woo, S.; Stuparu, M. C.; Bang, J.; Khan, A. Self-Assembly of an Interacting Binary Blend of Diblock Copolymers in Thin Films: A Potential Route to Porous Materials with Reactive Nanochannel Chemistry. *Soft Matter* **2014**, *10* (31), 5755−5762.

(25) Mulvenna, R. A.; Weidman, J. L.; Jing, B.; Pople, J. A.; Zhu, Y.; Boudouris, B. W.; Phillip, W. A. Tunable Nanoporous Membranes with Chemically-Tailored Pore Walls from Triblock Polymer Templates. *J. Membr. Sci.* **2014**, *470*, 246−256.

(26) Li, C.; Cho, J.; Yamada, K.; Hashizume, D.; Araoka, F.; Takezoe, H.; Aida, T.; Ishida, Y. Macroscopic Ordering of Helical Pores for

DOI: 10.1021/acs.macromol.7b00013
Macromolecules 2017, 50, 2777−2783

Arraying Guest Molecules Noncentrosymmetrically. *Nat. Commun.* **2015**, *6*, 8418.
(27) Lee, K. P.; Leese, H.; Mattia, D. Water Flow Enhancement in Hydrophilic Nanochannels. *Nanoscale* **2012**, *4* (8), 2621−2627.
(28) Wagener, K. B.; Boncella, J. M.; Nel, J. G. Acyclic Diene Metathesis (ADMET) Polymerization. *Macromolecules* **1991**, *24* (10), 2649−2657.
(29) Villazor, K. R.; Swager, T. M. Chiral Supramolecular Materials from Columnar Liquid Crystals. *Mol. Cryst. Liq. Cryst.* **2004**, *410* (1), 247−253.
(30) Wang, Y.; Poirier, R. A. Factors That Influence the CN Stretching Frequency in Imines. *J. Phys. Chem. A* **1997**, *101* (5), 907−912.
(31) Min, M.; Bang, G. S.; Lee, H.; Yu, B.-C. A Photoswitchable Methylene-Spaced Fluorinated Aryl Azobenzene Monolayer Grafted on Silicon. *Chem. Commun.* **2010**, *46* (29), 5232−5234.
(32) Su, X.; Bu, L.; Dong, H.; Fu, S.; Zhuo, R.; Zhong, Z. An Injectable PEG-Based Hydrogel Synthesized by Strain-Promoted Alkyne−azide Cycloaddition for Use as an Embolic Agent. *RSC Adv.* **2016**, *6* (4), 2904−2909.

DOI: 10.1021/acs.macromol.7b00013
Macromolecules 2017, 50, 2777−2783